JOURNAL OF COMPUTATIONAL PHYSICS 103, 465–471 (1992)

NOTE

A New Lagrangian Method for Steady Supersonic Flow Computation Part III. Strong Shocks

1. INTRODUCTION

This technical note is a continuation of the two earlier papers by the authors ([1, 2]; hereafter referred to as Part I and Part II, respectively) on the new Lagrangian method for two-dimensional steady supersonic flow computation.

In Part I the Godunov shock-capturing scheme was applied to the new Lagrangian formulation, and its potential advantages were demonstrated. Part II, on the other hand, applied a high resolution TVD scheme to the new formulation and shows that slip-line discontinuities are always resolved, with no special procedure for detecting them, in at most two grid points—a result clearly superior to the Eulerian formulation.

In this paper, Part III, we study two special difficulties associated with computing steady supersonic flow where strong shocks are present. These difficulties are inherited in the flow field and thus occur in both Lagrangian and Eulerian formulations, but can be tackled more easily in the new Lagrangian formulation.

The first difficulty involves the well-posedness of the Cauchy problem and arises when the principle of domain of influence for the governing hyperbolic Euler equations is violated during marching [3]. This principle is a general rule that includes the well-known CFL condition. In the Eulerian formulation this is signalled by one component of the flow velocity changing from supersonic to subsonic on crossing the shock although the actual flow may remain supersonic. This happens when the shock is strong enough, and it renders the Cauchy problem of marching an ill-posed problem. Based on the new Lagrangian formulation, we shall analyze the problem and present an easy-to-apply numerical remedy for overcoming it in Section 2.

The second difficulty occurs when the shock is extremely strong so that the numerical errors due to Godunov averaging of flow within a cell containing the shock cause the Riemann problem to have no solution. This will be discussed in Section 3 and, again, a simple remedy will be given for overcoming it.

2. WELL-POSEDNESS OF THE CAUCHY PROBLEM IN GAS DYNAMICS AND ITS NUMERICAL TREATMENT

In the new Lagrangian formulation [1], the Euler equations of a thermally and calorically perfect gas are expressed in the following conservation form

$$\frac{\partial \mathbf{E}}{\partial \tau}+\frac{\partial \mathbf{F}}{\partial \xi}=0, \tag{1}$$

where

$$\mathbf{E}=(K, H, Ku+pV, Kv-pU, U, V)^{\mathrm{T}}$$

$$\mathbf{F}=(0, 0, -pv, pu, -u, -v)^{\mathrm{T}}$$

with $U=\partial x/\partial \xi$ and $V=\partial y/\partial \xi$ describing the cell deformation rates; $K=\rho(uV-vU)$, the mass flux and $H=(u^2+v^2)/2+(\gamma/(\gamma-1))(p/\rho)$ the total enthalpy; u, v, p, and ρ are the x- and y-velocity components, pressure, and density. Here τ, the Lagrangian time, and ξ, the stream function, are the independent variables. An explicit shock-capturing scheme (Godunov or TVD) will march forward exactly in the flow direction (see [1, 2]).

The property of the Lagrangian system (1) that the physical flow is closely followed makes the well-posedness (numerically, the stability) analysis very easy and straightforward. Consider a computational cell (also a fluid particle) in Fig. 1a, where initial values are given along the time line OA. For the well-posedness of this local Cauchy problem of (1), the basic theory of hyperbolic equation (see Courant and Hilbert [3]) stipulates that OA must lie upstream of the domains of influence issuing from every point along OA; in particular, those fans from the end points O and A (shaded areas in Fig. 1a). This immediately leads to the following well-posedness (numerical stability) condition (or the general CFL condition),

$$\pi-\mu>\beta-\theta>\mu, \tag{2}$$

0021-9991/92 $5.00

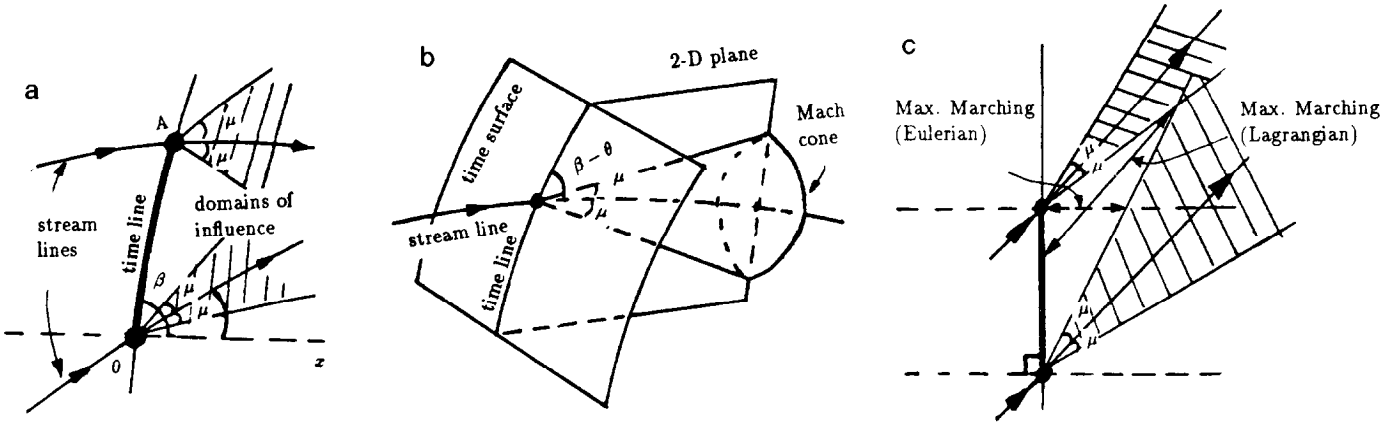

FIG. 1. (a) Domains of influence; (b) domain of influence for 3D flow; (c) comparison of CFL numbers.

where $\beta = \tan^{-1}(V/U)$ is the inclination of the time line vector $\mathbf{T} = (U, V)$, θ is the flow inclination angle, and μ is the local Mach angle.

When a supersonic gas flow passes through a strong shock, (2) could be violated due to the sudden jumps in θ and μ. Consequently, system (1) could become ill-posed and numerically instability take place. The criterion (2) immediately suggests a remedy: redirect the initial time line by properly choosing an initial β such that (2) is satisfied on both sides of the shock. Due to the flexibility of the time line, the redirection procedure can be performed even in the midst of computation without disturbing the formulation and any data already computed.

For demonstration of the simple remedy, we choose two examples and employ a high resolution TVD scheme as explained in Part II. With a naive choice of $\beta = 90°$ the numerical procedures soon blow up in both examples, no matter how small a time step size $\Delta\tau$ is chosen. Redirection of time line thus becomes necessary.

Example 1 is a Riemann problem formed with two intersecting streams as shown in Fig. 2. Twenty uniform cells with $h = 0.01$ are used for the top part and 30 non-uniform cells are used for the bottom part. The simple initial choice of $\beta_0 = 90°$ for both top and bottom parts of the flow field leads to failure as (2) is violated on the top part. But with $\beta_0 = 150°$ for the top part and $\beta_0 = 90°$ for the bottom part, successful results are obtained. These are shown (with square symbols) in Fig. 2 for the Mach number distribution along a typical time line. Agreements with exact analytic solutions (shown with solid lines) are seen to be excellent. Both shock and slip-line discontinuities are captured in one grid point.

In example 2 we compute a supersonic flow past a given shape for which experimental results are obtained by Johannesen [4]. The forward portion of the body shape used in [4] consists of a straight line segment OA making an expansion angle of 5.1° to the oncoming supersonic

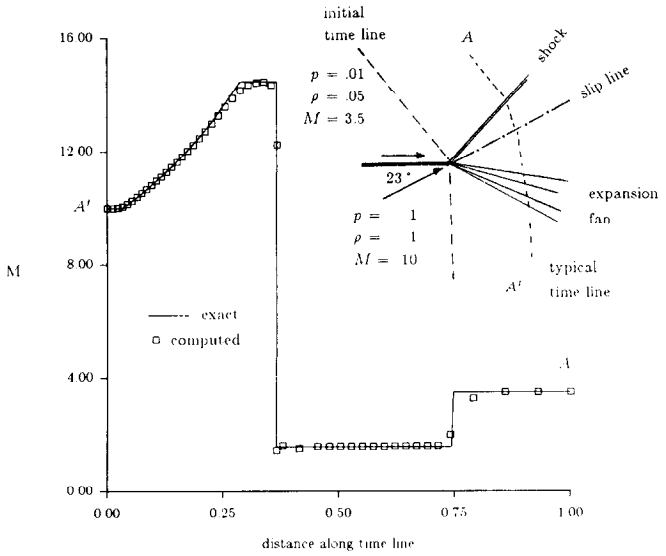

FIG. 2. Mach number along a typical time line in the Riemann problem with a strong shock.

stream M_∞ followed smoothly by a circular arc AB. The rear portion BD of the body shape is not specified in [4]. But as it produces an expansion flow and hence does not affect the flow upstream in an inviscid computation, we replace this part by a circular arc BC followed by a straight line CD. In the computation 125 uniform cells are used with $h = 0.02$, and $\Delta\tau = 0.000625$. Again the simple choice of $\beta_0 = 90°$ fails but $\beta_0 = 120°$ proves succesful. In Fig. 3a computed Mach number contours to be compared with Johannesen's experimental results are plotted and reproduced here as Fig. 3b. The agreement is seen to be excellent in practically every aspect of the flow field: the Pradtl–Meyer expansion fan, the converging Mach lines, the floating shock, and the vortex sheets downstream of it.

With the new Lagrangian formulation, the above well-posedness analysis can be easily extended to 3D flows

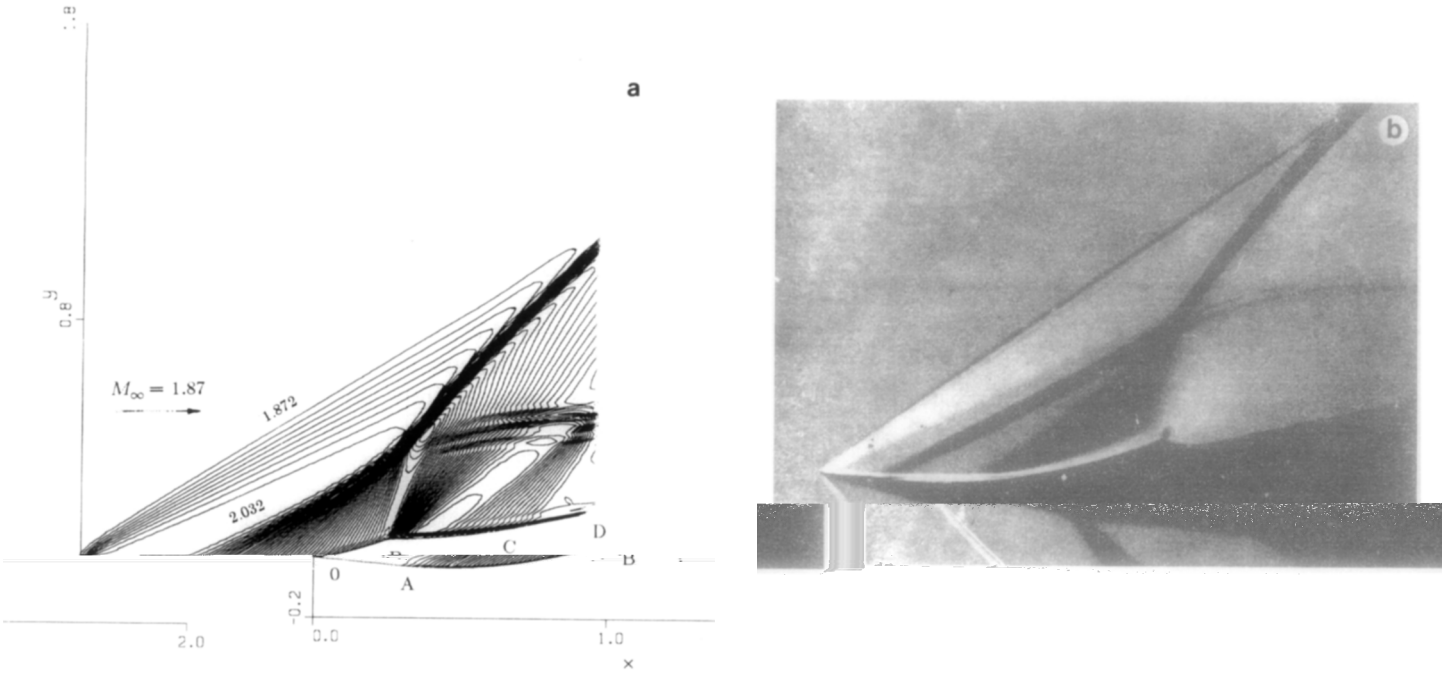

FIG. 3. Computed supersonic flow compared with experiment: (a) computed isomachs; (b) Schlieren photograph of Johannesen's experiment.

(Fig. 1b). The criterion is that the time surface passing through any point A must lie upstream of the Mach cone issuing from A (the domain of influence).

In the Eulerian formulation, the situation is similar to the case $\beta = 90°$ (with τ direction fixed). Then the only choice for resuming stability is to rotate the reference frame. Marconi and Morretti [5] employ a local coordinate rotation to their non-conservative implicit shock-fitting scheme to assure the proper domain of dependence of grid points with supersonic velocity in the overall marching direction. Obviously, their method is much more complicated than our simple method of redirecting a time line in the new Lagrangian formulation, particularly when conservation form and shock-capturing scheme are involved.

In addition, it is interesting and worth pointing out another advantage of the new Lagrangian formulation over its Eulerian counterpart: the scheme may march forward with a larger CFL number. This is illustrated in Fig. 1c, assuming that the initial time line coincides with the y-axis. Krispin and Glaz [6] have a similar observation.

3. SHOCK-CELL SPLITTING TECHNIQUE

In this section we present a shock-cell splitting technique as animprovement of Godunov shock-capturing scheme for solving the Euler equations. The importance of this technique will be shown to grow with the strength of the shock and becomes indespensible for extremely strong shocks where the flow downstream of the shock is close to being sonic.

It is well known that Godunov scheme smears admissible discontinuities due to conservative cell-averaging. This smearing can be so severe and critical in the presence of a strong shock that the solution to the Riemann problem becomes non-existent. In order to overcome a similar problem in 1D hyperbolic conservation laws and to improve the accuracy across a strong discontinuity, Harten and Hyman [7] introduce the self-adjusting grid method based on the Eulerian formulation. Here, for the same purpose, we introduce a method which we term the shock-cell splitting technique as the Lagrangian counterpart. The procedure is, however, different from Harten and Hyman's. We note that the Harten and Hyman method can resolve an

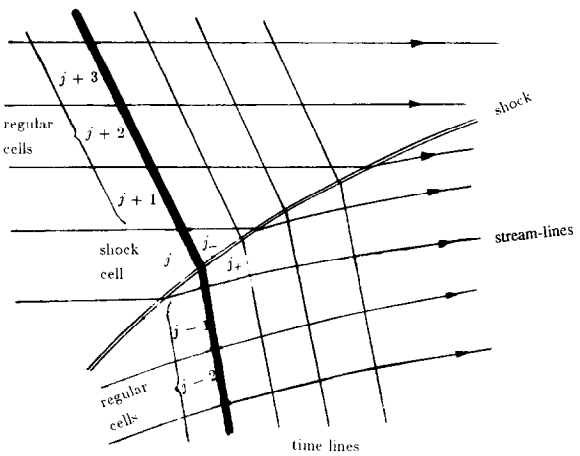

FIG. 4. Shock-cells and regular cells.

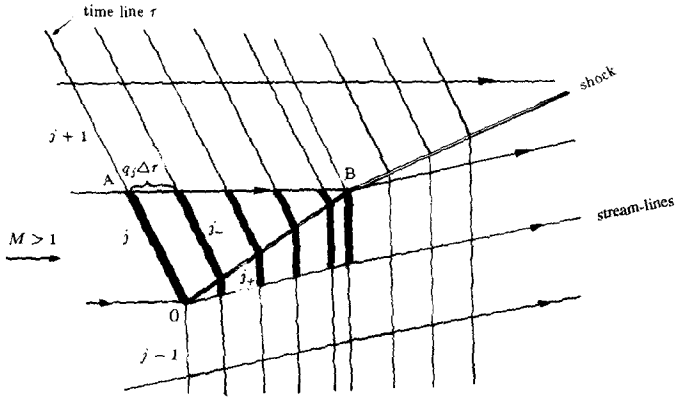

FIG. 5. Shock-cell splitting technique.

isolated shock or an isolated shock or an isolated slipline sharply but would be difficult to do so when a slipline intersects a shock. By contrast, sharp resolution of sliplines is already a property of the new Lagrangian formulation (Part II) and we need only to improve the resolution of shocks.

We assume that the location of the shock is initially known, e.g., boundary shocks originating from the leading edge or trailing edge of an airfoil, or at the engine inlet, or from a compression corner.

A computational cell is called a shock-cell when it contains both the upstream and the downstream part of the shock. Cells lying entirely on one side of the shock,

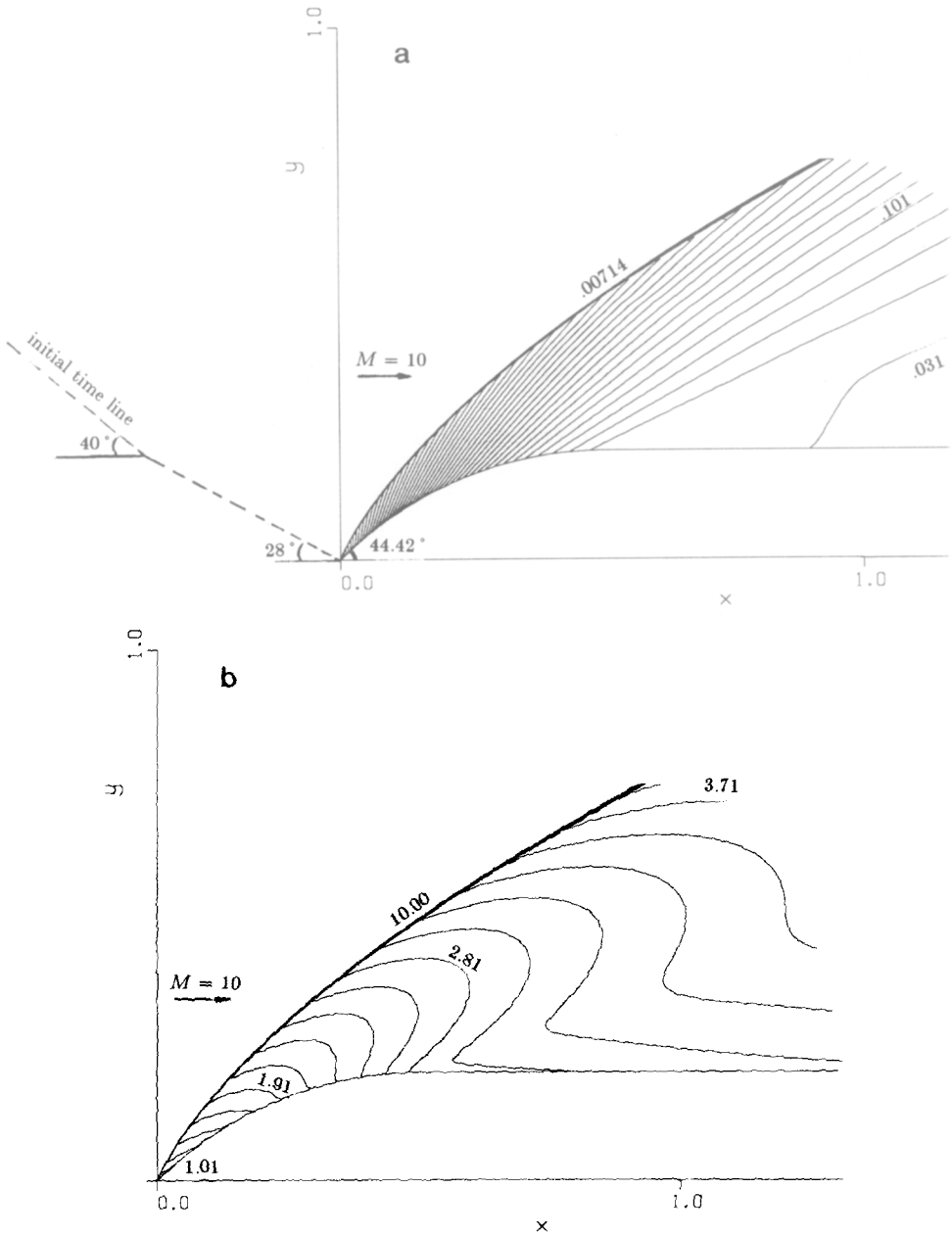

FIG. 6. Isobars for a $M = 10$ flow past an ogive, Godunov scheme with shock-cell splitting technique.

upstream or downstream, will be referred to as regular cells (Fig. 4). A major source of error in the Godunov scheme arises in averaging the flow within a cell that varies greatly across the cell, e.g., the discontinuous flow in a shock-cell. We therefore propose that it be improved by splitting the shock cell into two subcells j_- and j_+: the j_- cell lying entirely upstream of the shock and the j_+ cell, entirely downstream. They are then treated as ordinary cells in the usual way in the Godunov method. Within each subcell the flow is continuous and the Godunov-averaged uniform flow of each subcell is a good approximation for that subcell.

The details of this shock-cell splitting technique are as follows. Suppose it is known that a shock originates at the point 0 (Fig. 5), say, 0 being the leading edge of an airfoil. Over a time step $\Delta\tau$, which is determined by the CFL stability conditions for all the cells except cell j, the fluid particles on the upper part of cell j have advanced a distance $q_j \Delta\tau$, where q_j is the speed of the on-coming stream, while those on the lower part of the cell j advance a different distance due to a slower speed downstream of the shock. We thus split the cell j at the shock into two subcells: the upstream subcell j_- and the downstream on j_+. We use the flow state $\mathbf{Q}_j$ (i.e., u_j, v_j, p_j, and ρ_j) which is known at this stage along the time line τ, as the state $\mathbf{Q}_{j_-}$ of the upstream subcell j_-. The state $\mathbf{Q}_{j_+}$ of the down stream subcell j_+ and the shock angle δ_0 at 0 are obtained from the solution to the Riemann problem based on flow states $\mathbf{Q}_j$ and $\mathbf{Q}_{j-1}$ (or from the boundary Riemann problem if cell j is boundary cell). From the solution we also calculate U_{j_+} and V_{j_+}. During the subsequent marching in τ, the influences of the two subcells j_+ and j_- on their respective neighbouring cells $j+1$ and $j-1$ are computed through the Riemann problem in the usual way with subcells j_+ and j_- treated as regular cells, but the two subcells states $\mathbf{Q}_{j_-}$ and $\mathbf{Q}_{j_+}$ themselves, as well as (U_{j_-}, V_{j_+}), are kept unchanged. This marching proceeds until the streamline from the upper boundary A of the shock cell intersects the shock at B. (The location of B is determined from the known states $\mathbf{Q}_{j_-}$ and $\mathbf{Q}_{j_+}$ and the shock angle δ_0 through simple geometrical relation. Simultaneously, with each advance $\Delta\tau$ in time the j_+ subcell (downstream of shock) grows in size while the j_- subcell shrinks. This process is repeated until the j_- subcell size shrinks to exactly zero—this is made possible by suitably reducing the last time step $\Delta\tau$ so that the time line hits the shock exactly at B, where AB is a streamline. The upgrading to high resolution TVD accuracy applies to all regular cells except that shock-cell and the four adjacent cells: $j+2, j+1$, $j-1, j-2$. When the j_- subcell just disappears (i.e., when B is reached), the downstream subcell j_+ becomes a regular cell j and $\mathbf{Q}_{j_+}$ becomes the new $\mathbf{Q}_j$. However, to account for the influence of the cell $j-1$ on the shock-cell j during the previous time steps, the interaction between the cells j and $j-1$ is now computed through a Riemann solver (or a boundary Riemann solver if j is a boundary cell) and the newly coputed $\mathbf{Q}_j$ (including U_j and V_j) is used as the state $\mathbf{Q}_j$ for the new regular cell j. This completes a splitting process on one shock-cell. Then we continue to treat cell $j+1$ as a new shock-cell The cycle of shock-cell splitting can be repeated indefinitely.

The shock-cell splitting technique described above is equivalent to shock-fitting and hence gives exact solutions on both sides of the shock and resolves the shock crisply with its location off by at most one cell. Indeed, for supersonic flow past a compression corner, the shock-cell splitting technique reproduces the exact wedge flow. Like the shock-fitting method, it requires knowing the initial position of the shock. However, unlike the shock-fitting method, the shock cell splitting technique is embedded in the overall Godunov shock-capturing scheme and has no

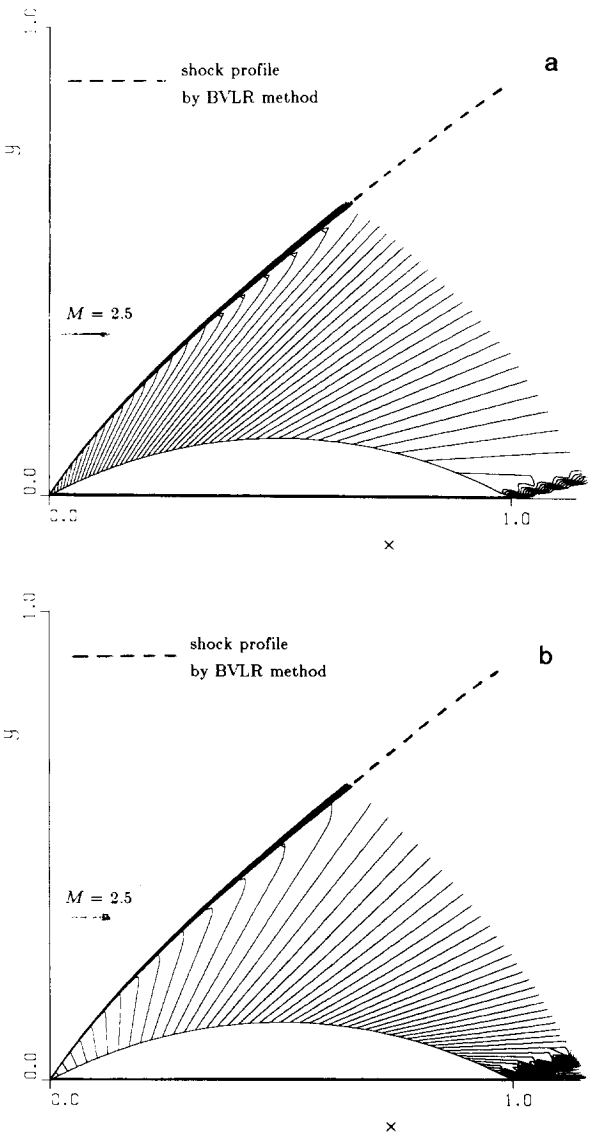

FIG. 7. Computed isobars for $M = 2.5$ supersonic stream past a thick airfoil, by Godunov scheme with shock-cell splitting technique.

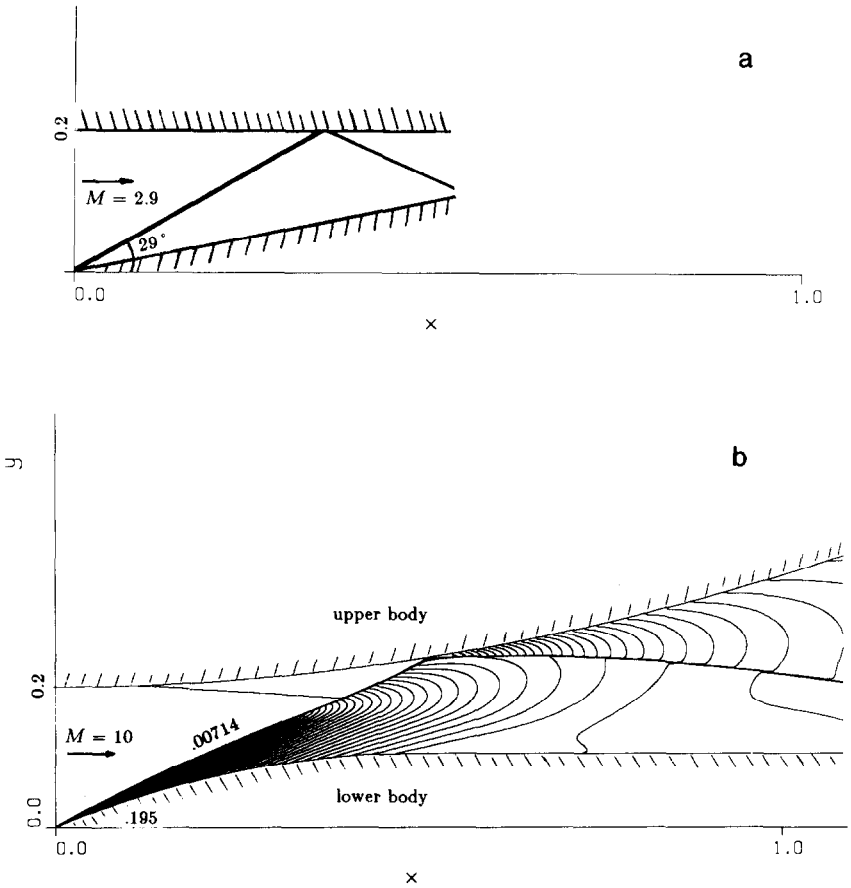

FIG. 8. Computed isobars in a shock reflection problem by Godunov scheme with shock-cell splitting technique.

additional difficulty in coding. Moreover, application of shock-cell splitting typically cuts down the computing time by about 30%, due to the rapid convergence of the iteration process in solving the Riemann problem across the shock.

We further remark that the need and the effectiveness of the shock-cell splitting technique increase with the strength of the shock. Weak shocks are captured quite well by the Godunov scheme without a shock-cell splitting technique; they are also notoriously difficult to detect and hence difficult to do shock-cell splitting. Extremely strong shocks, on the other hand, which the Godunov scheme might fail to capture, can be captured very well with the shock-cell splitting technique since they can be detected relatively easily.

When the shock-cell splitting technique is applied the shock is resolved accurately (to infinite order so to speak!) with its location possibly off by at most one cell. A first-order Godunov scheme combined with this technique is therefore expected to yield results with high accuracy. This indeed has been confirmed by our numerical experiments compared with the second-order TVD schemes. In Figs. 6–8, only the first-order results are presented.

The example in Fig. 6 is a hypersonic flow at $M = 10$ past an ogive; the leading edge and angle of the ogive is 44.42°. The standard Godunov or TVD scheme (Parts I and II) fails to converge for this problem, whilst the shock-cell splitting technique works very well and produces a crisp shock profile.

Figure 7 illustrates the isobars of a $M = 2.5$ flow past a thick airfoil. The same problem was solved by Holt [9] with a BVLR shock-fitting method. It is observed that the bow shock profiles agree very well. The tail shock is captured in a regular way.

Figure 8 shows the computed isobars for the inlet flow at a turbo machine, with $M = 10$. Both incipient curved shock and reflected curved shock are seen resolved crisply.

ACKNOWLEDGMENTS

This research was supported by the National Science and Engineering Research Council of Canada.

REFERENCES

1. C. Y. Loh and W. H. Hui, *J. Comput. Phys.* **89**, 207 (1991).
2. W. H. Hui and C. Y. Loh, *J. Comput. Phys.* **103**, 350 (1992).

3. R. Courant and D. Hilbert, *Methods of Mathematical Physics, Part II* (Wiley, New York, 1962).
4. N. H. Johannesen, *Philos. Mag.* **43**, 568 (1952).
5. F. Marconi and G. Moretti, AIAA Paper No. 76-383, 1976.
6. J. Krispin and H. Glaz, AIAA Paper No. 91-1653, 1991.
7. A. Harten and J. M. Hyman, *J. Comput. Phys.* **50**, 235 (1983).
8. S. K. Godunov, *Mat. Sb.* **47**, 271 (1959).
9. M. Holt, *Numerical Methods in Fluid Dynamics* (Springer-Verlag, New York, 1977).

Received June 7, 1990; revised July 29, 1991

W. H. Hui
Department of Applied Mathematics
University of Waterloo
Waterloo, Ontario, Canada N2L 3G1

C. Y. Loh
Mail Stop 5-11, NASA Lewis Research Center
Cleveland, Ohio 44135